MAGNETIC RESONANCE VELOCIMETRY IN COMPLEX TURBULENT INTERNAL FLOWS

Christopher J. Elkins, John K. Eaton
Department of Mechanical Engineering, Stanford University
Stanford, California 94305-3030, USA
elkins@vk.stanford.edu, eaton@vk.stanford.edu

Michael Markl, Norbert Pelc
Department of Radiology, Lucas MRI/S Center
Stanford, California 94305-5105, USA
markl@s-word.stanford.edu, pelc@stanford.edu

ABSTRACT

The aim of this paper is to apply a technique called 4D magnetic resonance velocimetry (4D-MRV) to measure the mean flow in a model of a gas turbine blade internal cooling geometry with four serpentine passages for three different Reynolds numbers (10,000, 21,000, and 53,000) based on bulk mean velocity and hydraulic diameter. The Reynolds number effects in this flow are also investigated. 4D-MRV utilizes an adaptation of a medical magnetic resonance imaging system to non-invasively measure the three component mean velocity field in complex turbulent flows. 4D-MRV is capable of completing full field measurements in three-dimensional volumes with sizes on the order of the magnet bore diameter in less than 1 hour. Such measurements can include over 2 million independent mean velocity vectors. In the turbulent passage flow, the average flow rates calculated from the 4D-MRV velocity profiles agreed with flow measurements to within 4%. The measurements lend excellent qualitative insight into flow structures even in the highly complex 180° bends. Accurate quantitative measurements were obtained throughout the flows for all three Reynolds numbers. While the large features of the flow remain basically the same as the Reynolds number increased, many differences occur as well. In particular, the size of the separation region downstream of the bends and turbulators decreases slightly with increasing Reynolds number. The 4D-MRV measurements provide very detailed three-dimensional data ideal for comparing to CFD.

INTRODUCTION

Energy conversion devices typically include turbulent flows through complex internal geometries such as those found in heat exchangers, piping manifolds, and turbine cooling passages. Flows in these devices are characterized by multiple regions of flow separation and strong secondary flows. In order to understand such flows, three-component velocity data are needed at a large number of points. In the absence of such information, engineers are forced to design devices using educated guesses and conservative safety factors.

Even with the advances made in CFD and laser-based measurement techniques, three-component velocity data are difficult to obtain in complex geometries. CFD can provide such data, but requires enormous computer resources. Also, there continue to be difficulties in applying turbulence models in regions where the turbulence is strongly out of equilibrium, such as around separation bubbles. Laser based measurement techniques such as laser Doppler anemometry or stereoscopic and/or holographic particle image velocimetry can also provide the data. However, optical access requirements and measurement times make these techniques impractical for very complex flows.

Medical magnetic resonance imaging (MRI) systems provide an alternative method for making non-invasive velocity field measurements in complex turbulent internal flows. Elkins et al. (2003) present one such technique called 4D-magnetic resonance velocimetry (MRV). Here, 4D implies that the velocity field is resolved over all three space dimensions as well as phase for a periodic velocity field. This technique may be used to acquire time-averaged velocity information in a turbulent field with a steady mean flow.

Using MRI to make fluid flow measurements is not a new concept. It has been used for numerous studies of laminar flows in experimental models and living organisms, but relatively few studies have attempted to measure turbulent flows. Fukushima (1999) details several MRI fluid mechanics studies many of which apply to low Reynolds number multiphase flows or laminar pulsatile physiologic flows. Turbulent studies include flow through straight pipes (Li et al. 1994, Gatenby and Gore 1996) and through stenotic (partially obstructed) pipes (Ku et al. 1990, Oshinski et al. 1995, Siegel et al. 1996, Gach and Lowe 2000). Li et al. (1994) used a time-averaging technique to measure pipe flow for Reynolds numbers between 1200 and 9400. Their technique produced one-component mean streamwise velocity profiles and turbulence intensity, which they showed to be related to the time-averaged pixel intensity in an image representing a 2D space-velocity plane. Even though additional information such as the statistics

of the instantaneous velocities can be mapped onto the mean velocity profile as shown by Li et al., these results have been limited to flow in simple geometries.

Two of the previous studies attempted to study turbulence by shortening the total imaging time to approximately 10 milliseconds. Gatenby and Gore (1996) used echo-planar imaging (EPI) to study pipe flow for Reynolds numbers up to 6300, and Gach and Lowe (2000) used their rotating ultra-fast imaging sequence (RUFIS) to image turbulent flow through a 75% stenosis. These techniques are useful for capturing a snapshot of one component of velocity in a 2D plane, but they are not applicable to imaging three components of velocity in a complete 3D volume, primarily due to constraints presented by the required scan time.

At present, it is possible to acquire the average three-dimensional flow in a 3D volume in a very reasonable amount of time using the phase-contrast 4D (three spatial dimensions and time) sequence presented in Markl et al. (2002) and Elkins et al. (2003). Other similar 4D sequences have been used to image physiologic flows (Bogren and Buonocore 1999, Ebbers et al. 2001, Kozerke et al. 2001). MRV is based on a phase-contrast 4D sequence originally developed to study pulsatile physiologic flows, but it is easily adapted to the study of steady flow. The advantages gained from using 3D or 4D sequences to image flow in a 3D volume extend beyond saving time in data acquisition and reconstruction. A significant advantage is the ability to obtain high spatial resolution in all three dimensions with higher signal-to-noise ratio (SNR) compared to 2D methods at the same resolution.

Operating Reynolds numbers for the flow in gas turbine blade internal cooling passages typically range from about 10,000 to as high as 100,000. Experiments and simulations in these flows are conducted in the lower portion of this range, and there is a question as to how Reynolds number affects the flow features. Therefore, there is a need for full-field experimental data over a range of Reynolds numbers. Applications of MRV usually are limited to Reynolds numbers of about 10,000 or less, so it was not known if the technique could be applied in high Reynolds number turbulent flows.

The aim of this paper is to apply the 4D-MRV technique to measure the turbulent flow through a model of a gas turbine blade internal cooling passage for Reynolds numbers equal to 10000, 21000, and 53000 based on mean bulk velocity and passage hydraulic diameter. Not only do these data lend considerable insight into the complex structure of the flow in internal cooling passages, but the resolution of the measurements makes them appropriate for direct comparison with CFD results. Our intention is to provide these data to the turbulence community for qualifying CFD codes to be used in complex geometries. The data are appropriate for determining how well the code captures the mean behavior of the turbulent flow.

METHODS

Internal Cooling Passage Model

Three-component velocity data were acquired in a simplified model of the internal cooling passages used in gas turbine blades. These serpentine passages include sharp bends and angled ribs (also called turbulators) attached to two of the four channel walls. Figure 1 shows the model with a few of its important dimensions. The model includes angled ribs of square cross section and three bends with varied shapes. The inlet and outlet are converging and diverging nozzles, respectively. Each has a circular cross section of diameter 3.49 cm that contorts into the square cross section (2.0 cm by 2.0cm) of the passage over a distance of 3.8 cm. These nozzles facilitate the use of fully developed pipe flow for inlet flow conditions to provide a well-defined initial condition for use in comparing CFD results.

The model was drawn using SolidWorks and made out of 5220 resin with a 3D Systems 250-50 SLA machine in less than 24 hours. Clearly, a very large grid would be required for a well-resolved CFD study of this flow, and detailed full-field measurements using PIV would require stereoscopic measurements over a large number of measurement planes.

MR System and Sequence

Magnetic Resonance Imaging (MRI) is a technique for generating spatially resolved images inside an object utilizing static and gradient magnetic fields and radio frequency (RF) pulses. For a discussion of the principles of MRI, the reader is referred to Stark and Bradley (1999), von Schultess and Hennig (1998), and Haacke et al. (1999). In addition, a brief discussion of MRV principles is found in Elkins et al. (2003) where the 4D-MRV technique is described in detail.

All measurements were performed on a 1.5 Tesla system (Signa CV/i, GE, G_{max} = 40mT/m, rise time = 268μs). Images were acquired using a standard head coil for all experiments.

The 3D volume around the internal cooling passage model shown in Figure 1 was scanned with a slab thickness of 36 mm and a field of view (FOV) of 280 mm resulting in a volume with dimension 36 x 280 x 280 mm. An imaging matrix of 36 x 256 x 256 resulted in a pixel resolution of 1.0 x 1.09 x 1.09 mm. In the 10,000 and 21,000 Reynolds number cases, the sequence parameters were TE=1.9 ms, TR=5.9 ms, n_{kz} =6, flip angle=15° with a Venc factor of 250 cm/sec in all directions. In the Re=53,000 case, the sequence parameters were TE=1.8 ms, TR=5.2 ms, n_{kz} =6, flip angle=15° with a Venc factor of 620 cm/sec in all directions. In each case, six complete data sets were acquired over a period of 27 minutes. The six data sets were averaged to reduce noise.

Steady Flow Loop

A steady flow loop was set up using a centrifugal pump (Little Giant model no. TE-6MD-HC) to circulate water at a temperature of 30 °C. Gadolinium-based contrast agent (Omniscan, Nycomed, Inc.) was added in a concentration of 0.5 %. The average flow rates for the two lower Reynolds number cases were measured using the bucket and stopwatch method. The flow rates were 10 and 21 L/min. MRV places a few restrictions on the experimental setup due to the large magnetic field and the sensitivity to RF noise. The pump was placed approximately 3 meters from the magnet, and no other metallic parts were used in the loop. The Little Giant pump was tested for RF interference and was found to produce a minimal amount of noise in MR images.

After traveling approximately 2 m through 2.54 cm ID flexible tubing, the fluid entered a 2.3 m long rigid, straight, transparent polycarbonate pipe with 3.49 cm ID

to produce fully developed turbulent pipe flow at the inlet to the model.

RESULTS

Average flow rates were calculated by integrating the measured velocity profiles at several cross sections in the model and averaging. These values for the three Reynolds number cases were 9.6, 20.5, and 52.6 L/min. The standard deviation in each case was 0.4, 0.4, and 1.1 L/min, respectively. For the two lowest Reynolds number cases, these calculated values agreed to within 2.5% and 4%, respectively, of the measured flow rates.

Figure 2 shows 4D-MRV signal magnitude images for an image plane slightly below the top of the ribs on one of the passage walls. A case with no flow is compared with all three Reynolds number cases. Note that the turbulators are well resolved. Comparing the images with flow to the flow-off image gives an idea of the effect of flow on the signal magnitude. In the flow-off image, the signal magnitude is nearly uniform except, of course, inside the turbulators where there are no water molecules. In regions of high velocity fluctuations, the magnitude decreases because the turbulence causes dephasing of the signal in that region. This is seen in the reattachment lines behind the turbulators and the shear layers outlining the recirculation zones around the bends. Note that these features become more prominent as the Reynolds number increases.

It is difficult to present all of the interesting features of the flow field due to the large amount of data acquired and the complexity of the configuration. To illustrate the detail available in the data set and the Reynolds number effects, data from the region around the first bend will be presented for Reynolds numbers 10,000 and 21,000. The complete data sets are available from the authors for those interested. Cross-sections in each of the three coordinate planes are shown in Figures 3, 4, and 5. The positions of these planes are shown in Figure 1. Velocity vectors are shown for both Reynolds numbers. The velocities are normalized by the mean bulk velocity in order to facilitate the comparison. The black vectors correspond to Reynolds number 10,000.

Figure 3 shows a view of the flow around the bend and the separation bubble downstream of it in the midplane of the channel. The flow direction directly above the bend differs between Reynolds numbers. In the Re=21,000 case, the flow follows the bend more closely. In addition, the flow in the higher Reynolds number case has more of a positive x-wise component further around the bend (right side of the figure).

Figure 4 shows a view of the flow in the second passage at the level of the bend. Note the presence of secondary flow structures. In particular, there is a pair of corner vortices and a stagnation region at the right hand wall in the middle of the channel. In general, the structures in the flow are the same for both Reynolds numbers with the notable exception of the left hand region of the figure where the low Reynolds number vectors have small x-wise components.

Figure 5 is a view of the flow in and downstream of the bend in a plane close to the inside sidewall of the bend. The right half of the figure shows flow in the channel of the bend where the secondary flow vortices are quite similar between Reynolds number cases. The left half of the figure shows flow downstream of the bend where the bulk flow direction is right to left. In the middle of the channel, vectors point in the opposite direction indicating the recirculation zone. The reattachment point can be seen where the vectors turn to the left. The flow around the turbulators on the upper and lower walls points to interesting Reynolds number effects. On the top wall, the vectors from both Reynolds numbers are virtually the same. However, the flow over the bottom turbulator is quite different between Reynolds numbers. The separation region appears smaller for the Re=21,000 case.

The flow in the Re=53,000 case more closely agrees with the Re=21,000 data. The overall patterns of secondary flow structures and separation regions remains the same for all Reynolds numbers studied, differences of the same nature as shown and discussed above exist between the Re=21,000 and Re=53,000 case.

DISCUSSION

The magnitude images and vector plots illustrate the complex structure of the flow in these serpentine passages. In particular, the flow in and around the bends and turbulators can be especially difficult to predict. The 4D-MRV measurements presented in this paper provide a great deal of information about these regions. Moreover, the measurements are quickly obtained from scans which take less than 30 minutes. When coupled with rapid prototyping manufacturing, which is ideal for making MR compatible complex internal passage flow models, the 4D-MRV technique can be a powerful tool for studying these difficult flows in a very short time on the order of a day. However, it is currently not a mature measurement technique.

An estimate for the uncertainty in 4D-MRV measurements of the mean velocity in turbulent pipe flow is reported as +/- 3% in Elkins et al. (2003). This uncertainty was derived from basic relations for MRV and the observed velocity noise in the flow-off scan. However, these estimates inadequately captured the total uncertainty since errors as high as +/- 10% were observed. For the passage flow reported here, it is difficult to assign an accurate uncertainty value to the measurements. The value derived from MRV principles will be too small. A better estimate is +/- 10% in agreement with the error observed in the pipe flow measurements. However, the flow in this study is more complex than pipe flow. The presence of higher velocity fluctuations and strong acceleration around the bends most likely results in higher errors. At present, the authors are working to more accurately quantify the uncertainty in these regions of the flow.

The results showed that while the large features of the flow remain basically the same as the Reynolds number increased, many differences occur as well. In particular, the size of the separation region downstream of the bends and turbulators decreases slightly with increasing Reynolds number. The x-component of the flow in the region just after the bend (see the left side of Figure 4) continues to increase with Reynolds number as well. These observations are important in deciding the appropriate Reynolds number to study. If only the large characteristic features are important in a study, then lower Reynolds numbers can be used. However, if the exact features are important, then the flow should be studied at operational Reynolds numbers.

Finally, the 4D-MRV technique provides very detailed three-dimensional data ideal for comparing to CFD. Since CFD relies on models which have difficulty in regions of complex flow, the 4D-MRV data are quite useful as validation data.

CONCLUSIONS

We have applied an experimental technique called 4D-MRV to the study of flow in a model of a gas turbine blade internal cooling geometry with four serpentine passages. Three component mean velocities were obtained for three Reynolds numbers, 10,000, 21,000, and 53,000, based on mean bulk velocity and passage height. Measured velocities lend excellent qualitative and quantitative insight into flow structures even in the highly complex 180° bends. Some regions of flow reach an asymptotic state with Reynolds number while other regions do not. This indicates that these flows may need to be studied at operating conditions depending on the information of interest. The density of velocity measurements makes these data sets particularly useful for comparison with CFD calculations. For those interested, the data is available from the authors.

ACKNOWLEDGEMENTS

Financial support was provided by the Department of Energy as part of the ASCI program at Stanford University. Use of the facilities at the Richard M. Lucas Center for Magnetic Resonance Spectroscopy and Imaging is gratefully acknowledged. The flow model was manufactured by Professor Ryan Wicker and Mr. Francisco Medina at the University of Texas at El Paso.

REFERENCES

Bogren HG; Buonocore MH (1999) 4D magnetic resonance velocity mapping of blood flow patterns in the aorta in young vs. elderly normal subjects. *J Magn Reson Imag* 10: 861-869.

Ebbers T; Wigstrom L; Bolger AF; Engvall J; Karlsson M (2001) Estimation of relative cardiovascular pressures using time-resolved three-dimensional phase contrast MRI. *Magn Res Med* 45: 872-879.

Elkins, C; Eaton JK; Markl, M; Pelc, N (2003) 4D Magnetic Resonance Velocimetry for Mean Velocity Measurements in Complex Turbulent Flows. *Exp in Fluids*, accepted Jan 2003.

Fukushima E (1999) Nuclear magnetic resonance as a tool to study flow. *Ann Rev Fluid Mech* 31: 95-123.

Gach HM; Lowe IJ (2000) Measuring flow reattachment lengths downstream of a stenosis using MRI. *J Magn Reson Imag* 12: 939-948.

Gatenby JC; Gore JC (1996) Echo-planar-imaging studies of turbulent flow. *J Magn Reson A* 121: 193-200.

Haacke M; Brown R; Thompson M; Venkatesan R (1999) Magnetic Resonance Imaging. New York: Wiley-Liss.

Kozerke S; Hasenkam JM; Pedersen EM; Boesiger P (2001) Visualization of flow patterns distal to aortic valve prostheses in humans using a fast approach for cine 3D velocity mapping. *J Magn Reson Imag* 13: 690-698.

Ku DN; Biancheri CL; Pettigrew RI; Peifer JW; Markou CP; Engels H (1990) Evaluation of magnetic resonance velocimetry for steady flow. *J Biomech Eng.* 112: 464-72.

Li TQ; Seymour JD; Powell RL; McCarthy KL; Odberg L; McCarthy MJ (1994) Turbulent pipe flow studied by time-averaged NMR imaging: measurements of velocity profile and turbulent intensity. *Magn Reson Imag* 12: 923-34.

Markl M, Chan FP, Alley MT, Wedding KL, Draney MT, Elkins CJ, Parker DW, Wicker R, Taylor CA, Herfkens RJ, Pelc NJ (2002) Time Resolved Three Dimensional Phase Contrast MRI (4D-Flow). *J Magn Reson Imaging*, accepted November 2002.

Oshinski JN; Ku DN; Pettigrew RI (1995) Turbulent fluctuation velocity: the most significant determinant of signal loss in stenotic vessels. *Magn Res Med* 33: 193-199.

von Schulthess G; Hennig J (1998) Functional Imaging. Philadelphia, Lippincott-Raven; pp. 261-390.

Seigel JM; Oshinski JN; Pettigrew RI; Ku DN (1996) The accuracy of magnetic resonance phase velocity measurements in stenotic flow. *J Biomechanics* 29: 1665-1672.

Stark D; Bradley W (1999) Magnetic Resonance Imaging. St. Louis, Mosby-Year Book.

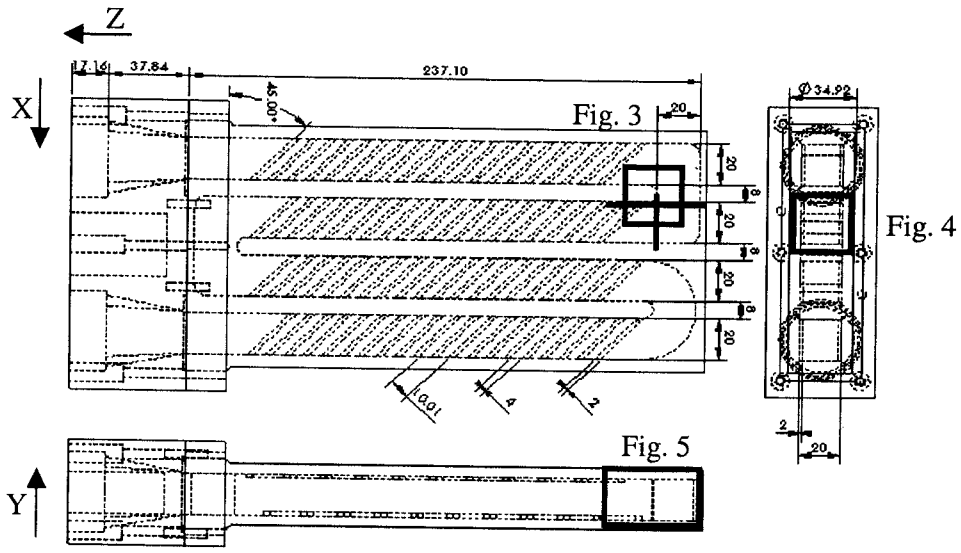

Figure 1: Drawing of the internal passage model (units=mm). Note the outlined regions indicate regions shown in Figures 3, 4, and 5. The labels indicate the corresponding figure number.

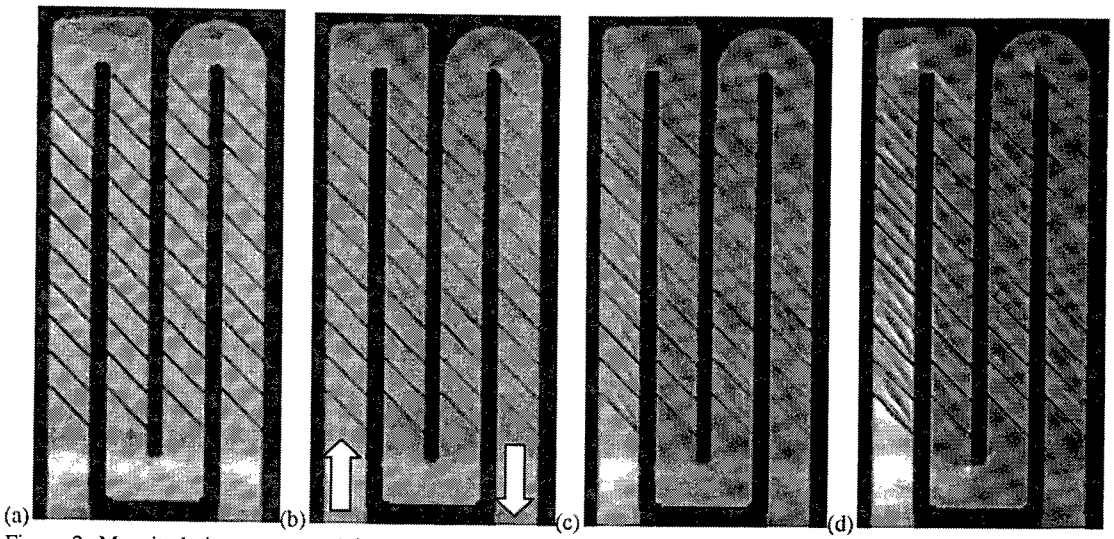

Figure 2: Magnitude images created from the 4D-MRV sequence for flow-off (a) and flow-on conditions for Re=10,000 (b), 21,000 (c), and 53,000 (d). Increasing brightness corresponds to increasing signal magnitude. Both images show slice planes at approximately the height of the turbulators. Flow features become more prominent as the Reynolds number increases. Arrows indicate flow direction.

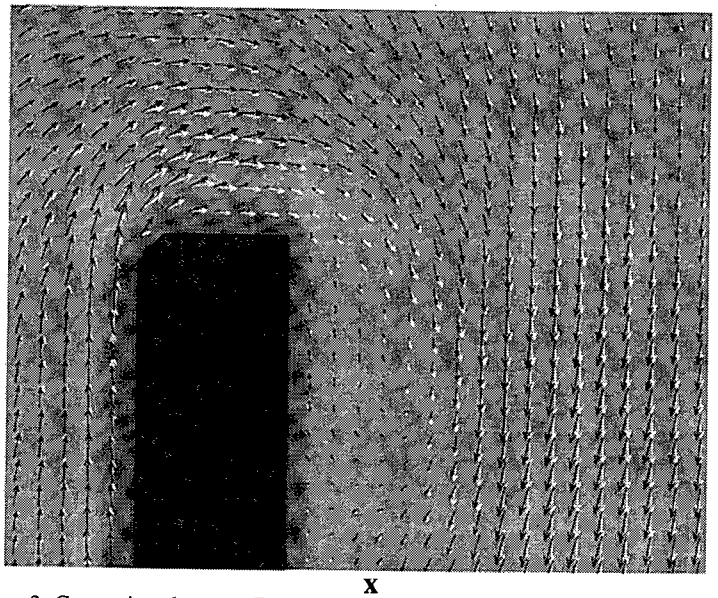

Figure 3: Comparison between Reynolds numbers 10,000 (black) and 21,000 (gray). In-plane velocity vectors at the mid height of the channel around the first bend. Note the presence of the recirculation zone in the bend. Point spacing is 1.1 mm.

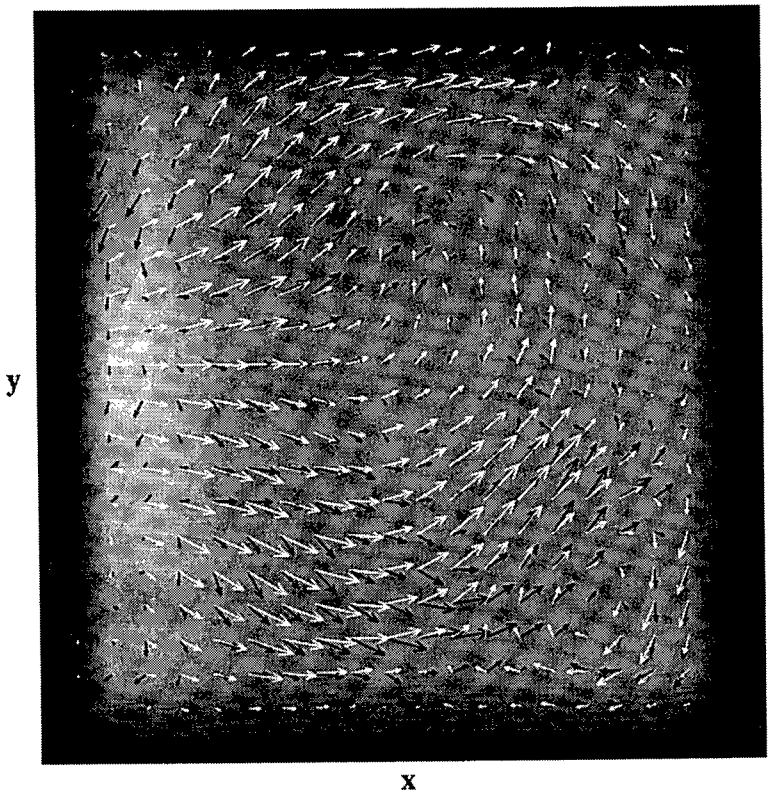

Figure 4: Comparison between Reynolds numbers 10,000 (black) and 21,000 (gray). In-plane velocity vectors in the second passage just downstream of the first bend. Note the presence of the corner vortices and the differences in flow on the left. Point spacing is 1.1 mm in X by 1.0 mm in Y.

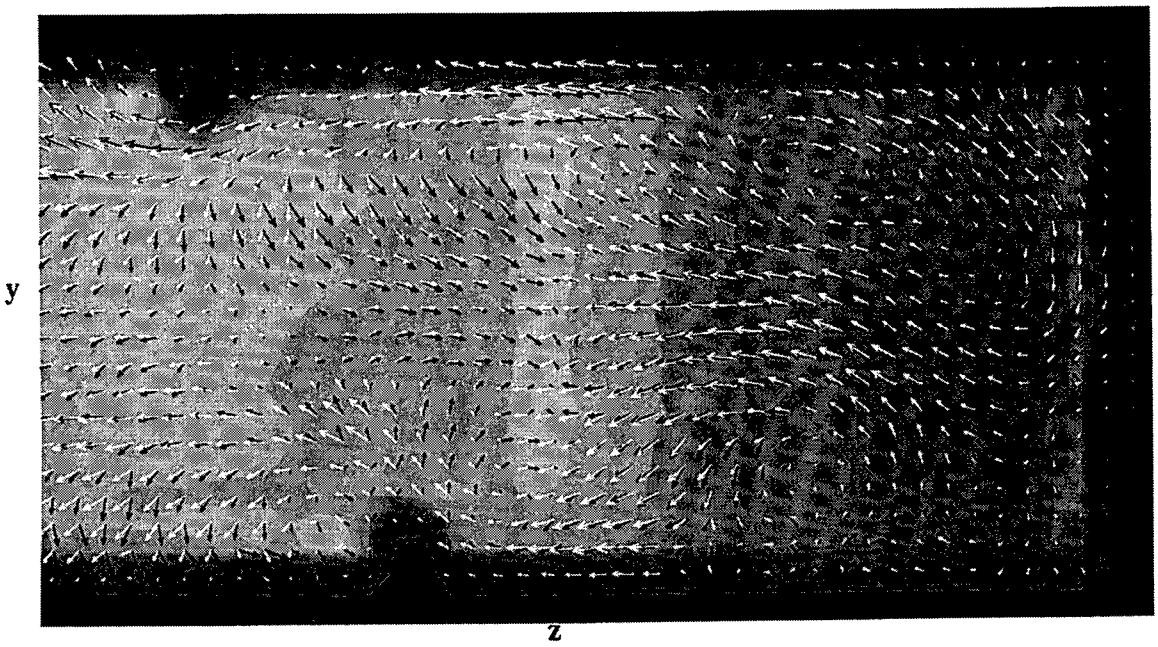

Figure 5: Comparison between Reynolds numbers 10,000 (black) and 21,000 (gray). In-plane velocity vectors in the first bend and second passage along the inside wall. Note the presence of the reverse flow in the middle of the channel to the left of the center of the figure. Flow around turbulators can be seen on the top and bottom of the figure. Point spacing is 1.1 mm in Z by 1.0 mm in Y.